SEMARAK ILMU PUBLISHING

Journal of Advanced Research in Numerical Heat Transfer

Journal homepage:
https://semarakilmu.com.my/journals/index.php/arnht/index
ISSN: 2735-0142

Numerical Analysis of Transient Convective Heat Transfer in a Dental Implant

Muhammad Ikman Ishak[1,*], Ruslizam Daud[1], Siti Noor Fazliah Mohd Noor[2]

[1] Fakulti Kejuruteraan & Teknologi Mekanikal, Universiti Malaysia Perlis (UniMAP), Kampus Alam UniMAP, Pauh Putra, 02600 Arau, Perlis, Malaysia
[2] Advanced Medical and Dental Institute, Universiti Sains Malaysia, Bertam, Jln. Tun Hamdan Sheikh Tahir, 13200 Kepala Batas, Pulau Pinang, Malaysia

ARTICLE INFO

Article history:
Received 21 February 2024
Received in revised form 20 March 2024
Accepted 25 April 2024
Available online 30 May 2024

Keywords:
Convection; Dental implant; Finite element analysis; Heat transfer

ABSTRACT

Hot substance consumption can have adverse effects on the neighbouring bone tissue in proximity to a dental implant. Elevated temperatures at the interface between the bone and implant could potentially disrupt the local cellular processes crucial for osteointegration. The primary goal of this study was to analyse the temperature and heat flux distributions within the implant body, surrounding bone, and bone-implant interface when the implant system subjected to a thermal load of transient nature. Transient thermal finite element analysis was utilised to analyse a three-dimensional model of dental implant with three different lengths – 6, 10, and 13 mm – placed in a mandible section. In order to obtain realistic results, thermal load was applied through convection on the outer surface of the prosthesis, simulating exposure to a hot liquid with the temperature and convection heat transfer coefficient of 67°C and 0.005 W/mm^2°C, respectively. The temperature of the other components in the model was maintained at a constant 37°C. The results showed that increasing the implant length generally led to lower temperature and heat flux levels in the implant body, bone, and bone-implant interface. The highest temperature and heat flux values were concentrated in the superior region, gradually decreasing toward the inferior region. Importantly, all maximum temperature values remained below the limits associated with cellular bone necrosis and remodelling, thereby reducing the risk of osteoporosis. It is noteworthy that, when considering transient thermal load, shorter implants pose a significantly higher risk of implant failure compared to longer ones.

1. Introduction

Consuming hot beverages and foods can potentially harm the tissues surrounding a dental prosthesis due to the contrasting thermal properties of natural teeth and replacement dental implants. Unlike natural teeth, which have built-in heat-resistant layers of dentin, enamel, and periodontal ligaments, dental implants often incorporate highly conductive materials, resulting in different thermal reactions [1, 2]. Typically composed of stainless steel or titanium, the threaded root

* *Corresponding author.*
E-mail address: ikman@unimap.edu.my (Muhammad Ikman Ishak)

https://doi.org/10.37934/arnht.20.1.112

of the implant is securely placed into the jawbone. Alongside its proximity to the metal root, certain specialised mechano-physiological functions elevate the significance of bone cells compared to other oral tissues, with bone remodelling being the most prominent among them.

The stability of a dental implant heavily relies on osteointegration with the surrounding area [3, 4]. This process involves an uptick in bone density near the implant site, facilitated by the activation of osteoblast cells, which in turn bolsters the implant's anchoring and improves its chances of long-term success. Under normal circumstances, these cells are naturally recruited to form bone unless there are underlying disorders or extreme external conditions [5], such as excessive mechanical overloading or unloading of the implant [6], or frequent exposure to high temperatures [7]. Daily and repetitive exposure to heat, as occurs when consuming hot beverages or eating piping-hot foods, can potentially have a detrimental impact on the osteointegration process.

While substantial published works predominantly centres on the natural teeth, specifically focusing on the tooth layers and their connections, there is a notable scarcity of data concerning bone temperature. Excessive heat occurring at the interface between the bone and implant can lead to irreversible bone damage, jeopardizing the process of osseointegration [8]. Research has indicated that bone necrosis typically occurs at temperatures exceeding 47°C [9, 10], and even a thermal impulse as low as 42°C can cause severe damage to osteoblasts [11]. Li *et al.,* have asserted that a thermal impulse of at least 42°C can temporarily disrupt the functioning and vitality of osteoblasts [11]. An *in vitro* study has also been conducted to measure the heat generated at the bone-implant interface resulting from the exothermic reaction of two impression plasters [12]. The results showed that the temperature increase is more prominent at the implant's coronal than at its apical part. Additionally, Feuerstein *et al.,'*s experimental work has revealed that the highest temperature values are concentrated near the abutment, while the apical and mid-length regions of the bone-implant interface experience comparatively lower temperatures that still exceed vitality thresholds [13]. A more recent study by Rabbani Arshad *et al.,* employed a transient heat transfer analysis and reported that the use of a ceramic crown resulted in the diffusion of heat into the deeper parts of the implant and the surrounding bone [7]. Interestingly, the model without a crown component yielded significantly lower temperature values compared to the experiments under the same conditions.

Computational heat transfer, coupled with thermal loading analysis using the finite element method (FEM), has emerged as a powerful tool in engineering. This interdisciplinary approach allows engineers to simulate and understand complex thermal behaviours within structures, devices, or systems [14, 15]. By employing FEM, which discretizes the geometry into finite elements, numerical solutions can be derived for heat transfer equations, offering insights into temperature distributions, thermal gradients, and potential hotspots. These simulations help optimize designs, ensuring components withstand thermal stresses and preventing overheating issues. Moreover, experimental validation plays a crucial role in corroborating computational results, enhancing the reliability of the analysis. This integrated approach not only accelerates the design process but also facilitates the development of robust and thermally efficient systems across various industries, from electronics to aerospace [16].

The primary aim of this study is therefore to employ finite element analysis to assess transient convective heat transfer within dental implants of varying lengths that have been implanted in the mandibular bone segment. Finite element analysis (FEA) is widely used in engineering and structural design to simulate and analyse complex systems, aiding in the optimisation of designs and ensuring their safety and performance. It finds applications in various fields such as aerospace, automotive, and biomechanics, enabling precise predictions of how structures and materials will behave under different conditions [17-19]. The source of thermal load introduced in this study originates from the routine consumption of hot substances. The outcomes of study were presented through the

determination of maximum temperature levels and heat flux values occurring within the implant structure, the surrounding bone tissue, and the interface between the bone and implant. A hypothesis being tested is whether the habitual consumption of hot substances might potentially compromise the integrity of the implant and surrounding bone, and consequently influence the process of osteointegration.

2. Materials and Methods

2.1 Geometric Model Reconstruction

A three-dimensional (3-D) model of the lower jaw (mandible) was developed based on computerised tomography images scanned data. The data was then transferred to visual processing software, Mimics 20.0 (Materialise, Leuven, Belgium). The process of isolating the compact and trabecular bones relied on the use of Hounsfield units. The study primarily centred on the posterior section of the left mandible, covering the areas associated with the second premolar, first molar, and second molar as exhibited in Figure 1(a). It is worth mentioning that the study did not include an examination of the mandibular canal. Comprising a section of edentulous, posterior mandible classified as type II according to Lekholm and Zarb's classification, the generated model featured an outer layer of the cortical bone, measuring approximately 2 mm in thickness, encompassing a dense trabecular bone core. To generate a more intricate 3-D geometric model of the mandible, the data was exported to the SolidWorks 2020 software (SolidWorks Corp., Concord, Massachusetts, USA) for additional refinement. As part of this process, the upper section underwent refinement to address the possibility of significant distortion in the mesh in that particular area. After the process was finished, the mandibular bone model that emerged had dimensions of 30 mm in length, a height of 20 mm, and a width ranging from 8 to 10 mm. The dimensions aligned with those documented in prior numerical studies concentrating on the identical regions of interest [20, 21].

For the purpose of simulating the implant insertion into the bone, the model excluded the first molar tooth to represent a single tooth restoration and did not account for the presence of the two neighbouring teeth. A model resembling the anatomical structure of the first molar's enamel was produced through Boolean operations to serve as a representation of the prosthesis or crown. Furthermore, the metal framework was established by scaling down the dimensions of the prosthesis model proportionally, reducing them by roughly 30%.

This study exclusively employed the dual-fit implant (DFI) system manufactured by Alpha-Bio Tec (Petach Tikva), with no other implant systems under consideration. For the same purpose, SolidWorks software was once again utilised to construct the 3-D model of the implant body, abutment, and abutment screw. The implant body featured a 3.75 mm diameter. For the implant length, there were three varying lengths subject to examination in this study, specifically 6 mm (L6 - short), 10 mm (L10 - regular), and 13 mm (L13 - long) as shown in Figure 1(b). Besides, the implant's interface with the abutment included an internal hexagonal connection, while the implant's threading was designed in a V-shaped form. The height of the abutment measures 3.5 mm, whereas the abutment screw has dimensions of 8 mm in length and 2.2 mm in width. Figure 1(c) depicts the configuration of implant assembly in the bone model.

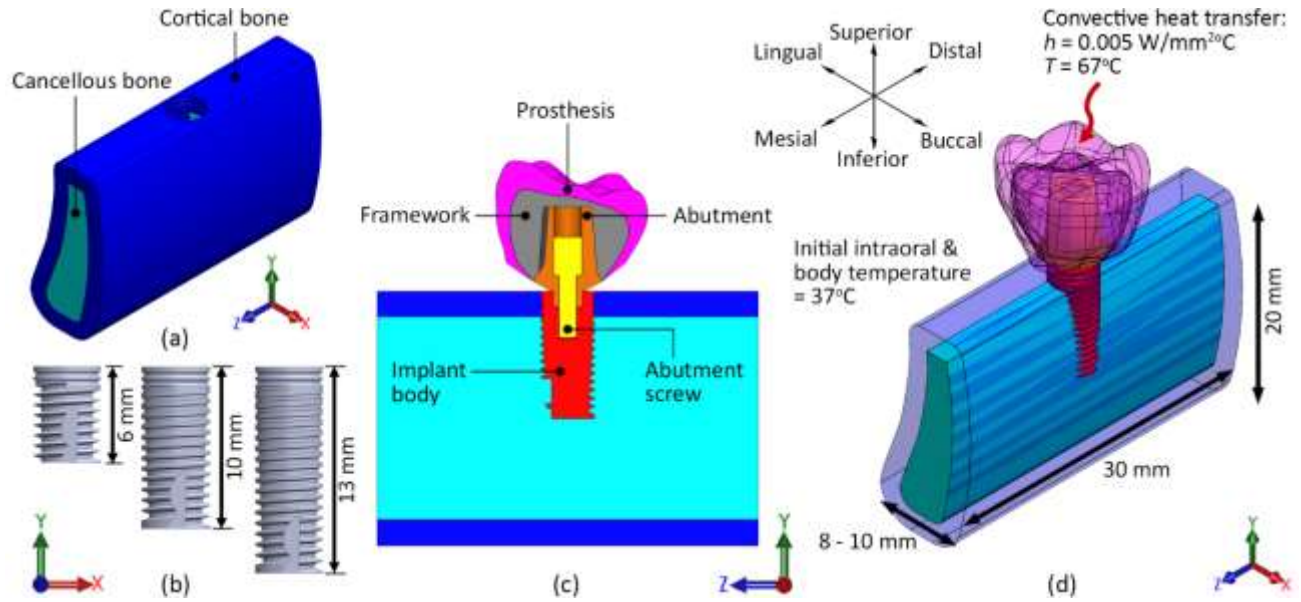

Fig. 1. (a) The cortical and cancellous bone models. (b) Implant body in different lengths – 6, 10, and 13 mm. (c) Assembly model of implant-bone. (d) Convective heat transfer imposed on the prosthesis of the model

Prior to conducting the implant insertion in the bone model, a step was taken to convert all the bone and implant component models into solid bodies. The chosen approach entailed bone-level implant placement, which was achieved by ensuring that the implant platform's flat surface was parallel to the uppermost cortical bone surface, thus maintaining a uniform elevation. This alignment played a crucial role in achieving the ideal orientation for the prosthesis. Through the application of the "Subtract" tool, we effectively established a 3.75-mm-wide bone bed for the implant placement.

2.2 Finite Element Analysis Pre-processing Settings

The materials selected for various implant components, including the implant body, abutment, and abutment screw, were assumed to be titanium alloy (Ti-6Al-4V). In contrast, the framework and prosthesis were assumed to be made of feldspathic porcelain. In all models, which encompassed both cortical and cancellous bones, the assumed material properties were isotropic, homogeneous, and demonstrated linear elasticity. Table 1 provides a comprehensive list of thermal properties, encompassing thermal conductivity (k) and specific heat (C_p), for all the materials under consideration in the analysis.

Table 1
The thermal properties of all materials used in the analysis

Material	Model	Thermal Conductivity, k (W/m°C)	Specific Heat, C_p (J/kg°C)	References
Ti-6Al-4V	Abutment, abutment screw & implant body	6.7	520	Babayi *et al.,* [22]
Feldspathic porcelain	Prosthesis & framework	1.5	1070	Babayi *et al.,* [22]
Cortical & cancellous bones	-	0.586	1350	Babayi *et al.,* [22]

It was postulated that the interface between the compact and trabecular bones exhibited perfect unity which modelled through bonded contact. The similar type of contact was also assigned to other contact surfaces existed among implant components. Employing the direct contact method to execute bonded contact modelling ensures the prevention of any potential relative motion at the interfaces.

In the context of thermal loading conditions, a constant temperature of 37°C is presumed for all entities involved [1]. Furthermore, an external temperature of 67°C [1] was introduced to the prosthesis surfaces to simulate the presence of hot liquid, thus initiating convective heat transfer (Figure 1(d)). The time-dependent profile of this convective heat transfer is illustrated in Figure 2 [1]. The heat transfer coefficient between the hot liquid and the prosthesis was set at 0.005 W/mm²°C [1].

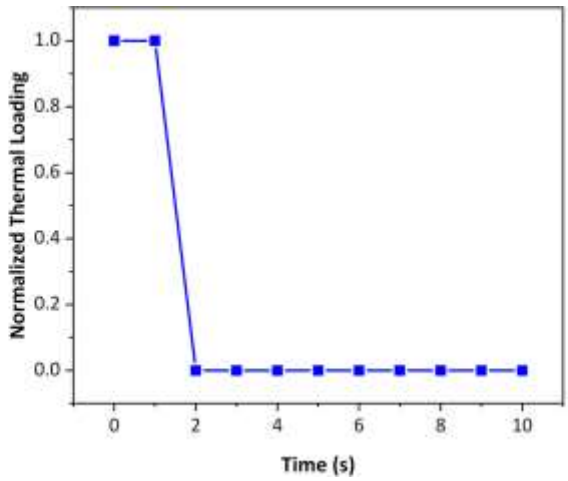

Fig. 2. Normalised thermal loading for the period of 10 seconds [1]

2.3 Mesh Convergence Test

A mesh convergence test was conducted to reduce the influence of purely numerical factors on the analysis results. To carry out this test, all geometric models were converted into finite element models using solid tetrahedral elements in the ANSYS software (ANSYS Inc., Houston, TX, USA). These tetrahedral elements are of the four-node type and offer three degrees of freedom. Six different mesh densities were prepared for the models, ranging from approximately 190,000 (Tet A: the lowest density) to 1,690,000 (Tet F: the highest density) elements. The mesh convergence test focused on assessing the maximum principal stress value recorded in the bone across all the models. The results revealed only a marginal difference in stress levels between the refined and coarser models. After just one refinement, the model demonstrated convergence with a mere 2.7% variation in the stress results. The converged model consisted of around 260,000 elements and 400,000 nodes. Figure 3 depicts the distribution of the maximum principal stress magnitude in all meshed models, along with the meshing elements generated in the refined and coarser models for comparison.

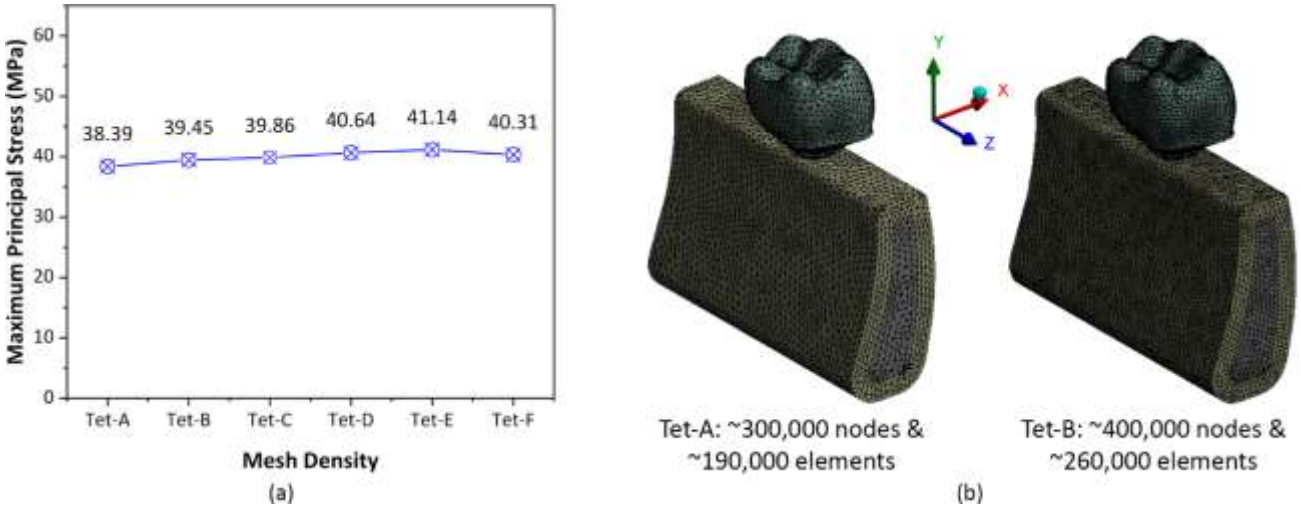

Fig. 3. (a) The maximum principal stress values across all the meshed models. (b) The comparison of tetrahedral elements distribution between the coarser (left) and more refined (right) models

2.4 Governing Equations

As the primary objective of this study revolves around examining heat transfer via conduction and convection, the fundamental governing equation we employ is the conservation of energy expressed in terms of temperature variations, specifically, the heat diffusion equation [1] as shown in Eq. (1).

$$\frac{\partial}{\partial x}\left(k\frac{\partial T}{\partial x}\right)+\frac{\partial}{\partial y}\left(k\frac{\partial T}{\partial y}\right)+\frac{\partial}{\partial z}\left(k\frac{\partial T}{\partial z}\right)+\dot{q}=\rho C_p\frac{\partial T}{\partial t} \tag{1}$$

In the given equation, the variables *x*, *y*, and *z* denote the Cartesian coordinates, while *k*, *ρ*, and C_p represent thermal properties, namely, the coefficient of thermal conductivity, density, and specific heat, respectively. In this equation, *T* represents temperature, which varies with both time and space. It is worth noting that the term $\dot{q}$, which signifies heat generation or absorption, is not considered in this study due to the absence of heat generation or dissipation.

The thermal energy input was transferred to the dental implant body through convection occurring between the material and the outer surface of the prosthesis, as described by the following equation, Eq. (2) [22].

$$q=hA\left(T_\infty-T_S\right) \tag{2}$$

In this context, *q* represents the thermal flux, *A* signifies the contact area, and *h* denotes the convection coefficient. Additionally, T_∞ corresponds to the temperature of the oral cavity when the hot substance is ingested, while T_S represents the temperature of the specific surface of interest, namely, the outer surface of the prosthesis.

3. Results

To ensure the attainment of significant results, we have considered two main heat transfer analysis result attributes which are the maximum temperature and heat flux values recorded within

the implant body, bone, and bone-implant interface to be evaluated. For the bone-implant interface, a pathway was defined starting from the superficial region and extending into the deeper areas. The interpretation of the findings was also supported by the colour contour plots of the result indices to clearly indicate the locations of critical and safe regions. Table 2 exhibits a summary of the results obtained from the analyses for all the three different implant lengths.

Table 2
The maximum values of temperature and heat flux recorded in the analyses

Results	Implant body			Bone			Bone-implant interface		
	L6	L10	L13	L6	L10	L13	L6	L10	L13
Temperature (°C)	41.13	40.29	40.28	39.78	38.51	38.46	39.74	38.35	38.37
Heat flux (W/mm^2)	0.25833	0.13896	0.1283	0.02439	0.01024	0.01096	0.00835	0.00538	0.00528

3.1 Temperature Distribution

Figure 4(a) demonstrates that an increase in implant length results in a corresponding decrease in the recorded temperature within both the implant body and the adjacent bone. The highest temperature was observed in L6 (41.13°C), followed by L10 (40.29°C), and L13 (40.28°C). Likewise, with regard to bone temperature, L6 exhibited the highest temperature level (39.78°C) when compared to the others (L10: 38.51°C and L13: 38.46°C). Notably, the temperature levels within the implant body were significantly higher than those within the bone, with differences of approximately 3.3%, 4.5%, and 4.6% for L6, L10, and L13, respectively.

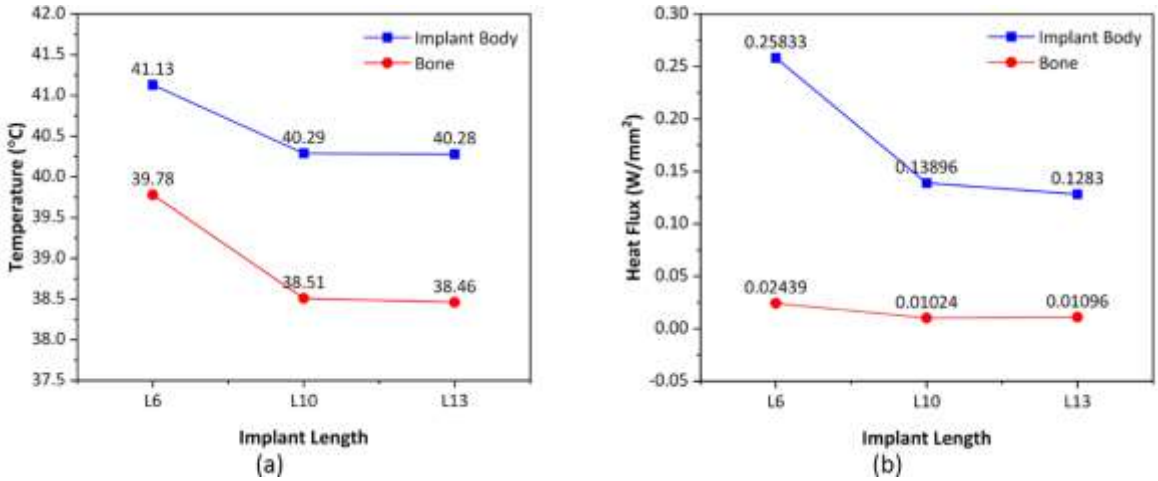

Fig. 4. The distribution of the maximum (a) temperature and (b) heat flux values within the implant body and bone

It is worth mentioning that regions of higher temperature were predominantly generated in the superior direction of both the implant body and the bone, particularly at the implant-abutment connection region, as illustrated in Figure 5. Among all the implant lengths, the L6 model exhibited a considerably wider area of elevated temperature compared to the L10 and L13 models. In the case of L6, high temperature was sustained nearly throughout the entire body, spanning from the superior to the inferior regions. Conversely, for L10 and L13 cases, concentrated temperature elevation was observed mainly at the top area, covering approximately half and one-third of the entire implant body structure, respectively. This observation aligns well with the temperature plots along a path at

the bone-implant interface, as shown in Figure 7(a). The plot illustrates a significant reduction in temperature levels, regardless of the implant lengths. The temperature of interface for all implants seemed to return to initial temperature, i.e., 37°C.

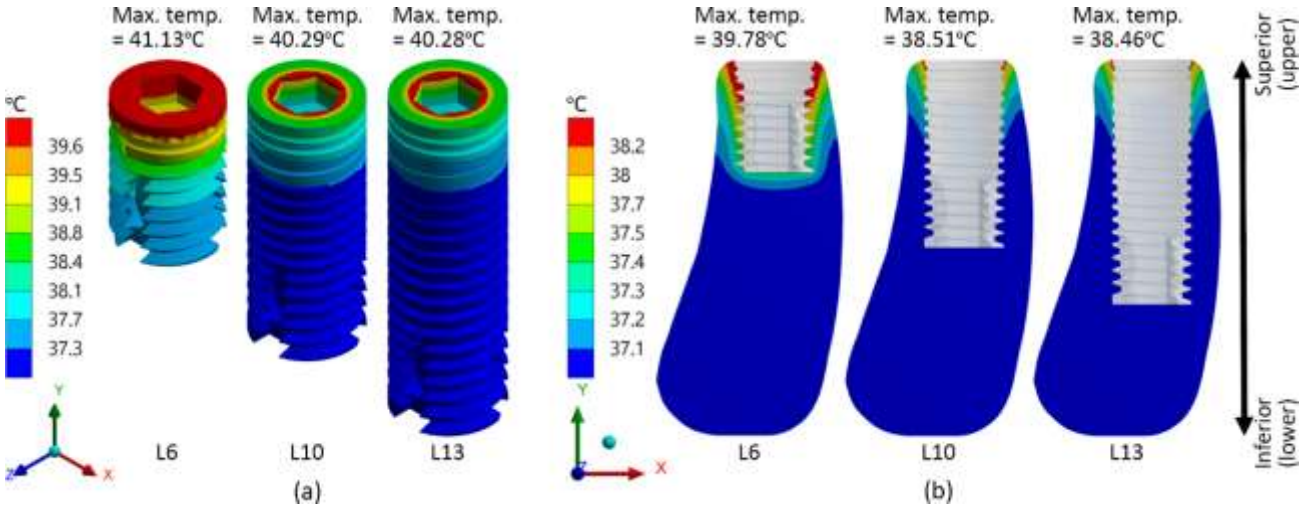

Fig. 5. The distribution of temperature levels within the (a) implant body and (b) bone (cross section)

3.2 Heat Flux Distribution

Concerning heat flux, it is noteworthy that the results generally align with the temperature penetration findings. An increased implant length corresponds to decreased heat flux levels in both the implant body and the surrounding bone, as depicted in Figure 4(b). In the case of the implant body, the highest value was 0.2583 W/mm² for L6, followed by 0.1389 W/mm² (L10) and 0.1283 W/mm² (L13). It is worth mentioning that heat flux in the bone was significantly lower than that in the implant body, regardless of implant length. Specifically, bone heat fluxes were 10.6 times lower for L6 (0.02439 W/mm²), 13.6 times lower for L10 (0.01024 W/mm²), and 11.7 times lower for L13 (0.01096 W/mm²) compared to those generated in the implant body.

In terms of the colour contour plots (Figure 6), it becomes evident that high heat flux accumulates at the edges of the implant-abutment connection, subsequently dispersing evenly towards the inferior region. This is parallel with the observations recorded for the bone, where the region surrounding the implant body, particularly the superior portion, endured a higher intensity of heat flux. Among the implant lengths, the shorter implant led to a less favourable heat flux distribution throughout the implant structure compared to the longer implant. Figure 7(b) supports this finding, showing that the 6-mm long implant exhibited a higher heat flux value relative to the 10-mm and 13-mm implants along the path at the bone-implant interface. In addition, heat flux magnitudes notably decreased as the path approached its end for all implant lengths.

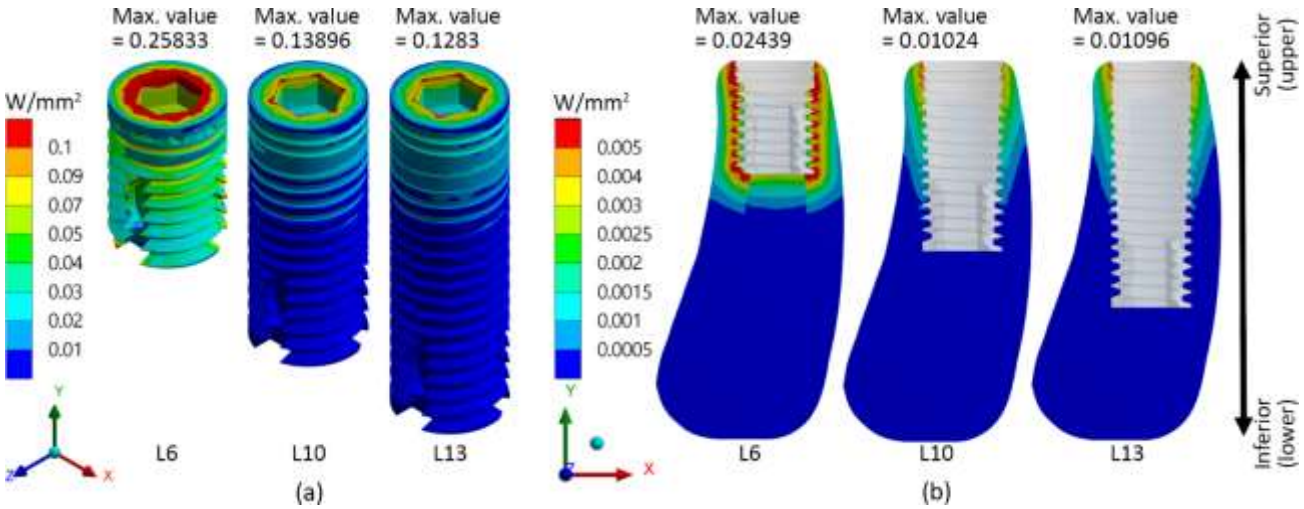

Fig. 6. The distribution of heat flux levels within the (a) implant body and (b) bone (cross section)

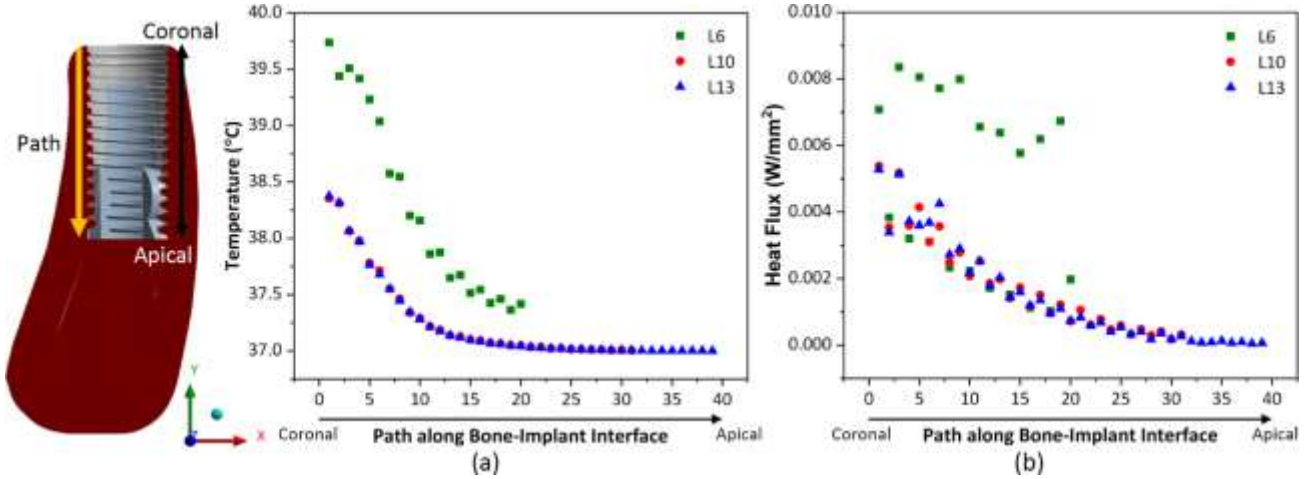

Fig. 7. The plot of (a) temperature and (b) heat flux changes along the path at the bone-implant interface

4. Discussion

In this study, finite element analysis was employed to investigate how heat is transmitted through convection when consuming hot substances in commercial dental implants of various lengths. One primary objective of the present study was to determine if the temperature increase in the adjacent bone surpasses the threshold for cell mortality, potentially impacting osteointegration. While the literature contains numerous studies exploring heat transfer through natural tooth structures [23], restorative materials [24], and the effects of drilling [25, 26] or laser-generated heat [27], research specifically addressing heat transfer in dental implants caused by hot beverages has been limited.

The relationship between bone quality at the bone-implant interface and implant stability was firmly established [22]. Enhancing bone density, whether cortical or cancellous, can occur through bone remodelling, which involves recruiting osteoblasts [6]. Beyond factors like mechanical stimulation or osteoblast deactivation, thermal loads, such as the consumption of hot beverages, have the potential to significantly elevate temperature levels experienced by the adjacent bone. The thermally conductive nature of titanium implants allows for rapid heat flux transfer from heat sources like the upper prosthesis or crown. It is noteworthy that, in this study, the prosthesis surface was thermally loaded at the maximum temperature of 67°C at the early stage of loading. The main findings showed that higher temperature and heat flux levels were evident in the superior region of the implant body, bone, and bone-implant interface. This phenomenon can be attributed to the

proximity of the superior region to the thermal source. As far as the temperature in the bone was concerned, the highest value recorded was 39.78°C (by the shortest implant, L6) that considerably lower than the necrosis of bone cell threshold of 47°C. Conversely, the middle and inferior regions of the bone-implant interface received less thermal energy, with temperatures dropping to a minimum of 37°C (by the longest implant, L13). It is important to highlight that all the peak magnitudes of temperature within the bone or interface did not exceed 42°C, the limit of bone remodelling intervention. Also, it is crucial to emphasise that heat flux input into the implant body differs from that in ceramic prostheses. Ceramics, characterised by their high specific heat coefficient and low conductivity, act as a barrier against heat transfer to the lower regions.

Concerning implant length, the shorter implant exhibited a more significant temperature decrease than the longer implant at the bone-implant interface. Nevertheless, the overall temperature levels remained considerably higher in comparison to those of the longer implant. This discrepancy can likely be attributed to the geometric configuration of the shorter implant body. It is evident that the shorter implant tends to accumulate higher temperature and heat flux throughout its body, rather than distributing them to the surrounding areas, as observed in the longer implants. For the longer implants, the middle region appears to primarily serve as an energy conduit, with a low likelihood of heat transfer from this region to the opposite side of the bone-implant interface. The region of elevated temperature does not extend far from the interface. Consequently, the inferior region remains in a stagnant condition. While the surrounding area maintains lower temperature and heat flux values than the critical thresholds, it can be inferred that most of the mandibular bone regions has been affected by the thermal stimuli.

The current discovery aligns with a previous study conducted by Rabbani Arshad *et al.,* which found that deeper regions of the bone exhibited lower temperature values (38.8°C) than the thresholds for vitality [7]. However, it is worth noting that the study omitted the prosthesis component, with thermal load directly in contact with the abutment and implant body. In contrast, a conflicting result emerged from the work of Feuerstein *et al.,* where the apical portion of the implant recorded a slightly higher temperature level, nearly reaching 45°C, as compared to our findings [13]. A similar pattern of results was also observed in a more recent study by Babayi *et al.,* where the implant's apical portion displayed greater susceptibility to bone necrosis, with a maximum temperature value of approximately 47°C [22]. Various factors could contribute to these discrepancies, including differences in heat source conditions, measurement locations, or even variations in implant design.

The present study encountered several limitations, with the most significant being the absence of neighbouring teeth or implants in the model. The lower jaw was represented as a solid segment of bone, receiving heat exclusively from a single thermally loaded prosthesis. Taking into account the heat flux from other teeth, even in their intact state, could have influenced the bone temperature. Additionally, the assumption of isotropic, linear, and homogeneous thermal and physical properties was made for all components, whereas biological tissues are inherently inhomogeneous in reality.

5. Conclusion

The finite element analysis of transient convective heat transfer on a dental implant with variation in the implant length supports the following conclusions.

i. The temperature and heat flux levels within the implant body, bone, and bone-implant interface were generally decreased as the implant length increased.

ii. More critical temperature and heat flux magnitudes concentrated at the superior region before being minimised towards the inferior region.
iii. All the maximum temperature values recorded were below the cellular bone necrosis and remodelling limits, therefore reducing the risk of osteoporosis.
iv. Of all implant lengths, the shorter implant is a significant factor predisposing to implant failure compared to the longer implant if transient thermal load is of concern.

Acknowledgement
The authors would like to acknowledge the support from Fundamental Research Grant Scheme (FRGS) under a grant number of FRGS/1/2020/TK0/UNIMAP/03/2 from the Ministry of Higher Education Malaysia. The authors reported no conflicts of interest related to this study.

References

[1] Ashtiani, M. N., and R. Imani. "Transient heat transfer in a dental prosthesis implanted in mandibular bone." In *26th Southern Biomedical Engineering Conference SBEC 2010, April 30-May 2, 2010, College Park, Maryland, USA*, pp. 376-379. Berlin, Heidelberg: Springer Berlin Heidelberg, 2010. https://doi.org/10.1007/978-3-642-14998-6_96
[2] Panotopoulos, Grigorios P., and Ziyad S. Haidar. "Thermal Load and Heat Transfer in Dental Titanium Implants: An Ex Vivo-Based Exact Analytical/Numerical Solution to the 'Heat Equation'." *Dentistry Journal* 10, no. 3 (2022): 43. https://doi.org/10.3390/dj10030043
[3] Dhok, Kanad, Mihir Adhikari, Atul Palange, and Pankaj Dhatrak. "Heat generation during implant site preparation and its effects on osseointegration: A review." *Materials Today: Proceedings* 72 (2023): 1035-1040. https://doi.org/10.1016/j.matpr.2022.09.157
[4] Liu, Yun-feng, Wu, Jian-lei, Zhang, Jian-xing, Peng, Wei, and Liao, Wen-qing. "Numerical and experimental analyses on the temperature distribution in the dental implant preparation area when using a surgical guide." *Journal of Prosthodontics* 27, no. 1 (2018): 42-51. https://doi.org/10.1111/jopr.12488
[5] Wood, Melanie R. and Vermilyea, Stanley G. "A review of selected dental literature on evidence-based treatment planning for dental implants: Report of the committee on research in fixed prosthodontics of the academy of fixed prosthodontics." *The Journal of Prosthetic Dentistry* 92, no. 5 (2004): 447-462https://doi.org/10.1016/j.prosdent.2004.08.003
[6] Lin, Daniel, Li, Qing, Li, Wei, Duckmanton, Naughton, and Swain, Michael. "Mandibular bone remodeling induced by dental implant." *Journal of Biomechanics* 43, no. 2 (2010): 287-293. https://doi.org/10.1016/j.jbiomech.2009.08.024
[7] Rabbani Arshad, Somayye, Zoljanahi Oskui, Iman, and Hashemi, Ata. "Thermal analysis of dental implants in mandibular premolar region: 3D FEM study." *Journal of Prosthodontics* 27, no. 3 (2018): 284-289. https://doi.org/10.1111/jopr.12486
[8] Aleisa, Khalil, Alkeraidis, Abdullah, Al-Dwairi, Ziad Nawaf, Altahawi, Hamdi, and Lynch, Edward. "Implant fixture heat transfer during abutment preparation." *Journal of Oral Implantology* 41, no. 3 (2015): 264-267. https://doi.org/10.1563/AAID-JOI-D-13-00056
[9] Eriksson, A. R., and T. Albrektsson. "Temperature threshold levels for heat-induced bone tissue injury: a vital-microscopic study in the rabbit." *The Journal of prosthetic dentistry* 50, no. 1 (1983): 101-107. https://doi.org/10.1016/0022-3913(83)90174-9
[10] Aquilanti, Luca, Antognoli, Luca, Rappelli, Giorgio, Di Felice, Roberto, and Scalise, Lorenzo. "Heat generation during initial osteotomy for implant site preparation: An in vitro measurement study." *Journal of Maxillofacial and Oral Surgery* 22, no. 2 (2023): 313-320. https://doi.org/10.1007/s12663-022-01800-8
[11] Li, Song, Chien, Shu, and Brånemark, Per-Ingvar. "Heat shock-induced necrosis and apoptosis in osteoblasts." *Journal of Orthopaedic Research* 17, no. 6 (1999): 891-899. https://doi.org/10.1002/jor.1100170614
[12] Nissan, J., D. Assif, M. D. Gross, A. Yaffe, and I. Binderman. "Effect of low intensity laser irradiation on surgically created bony defects in rats." *Journal of oral rehabilitation* 33, no. 8 (2006): 619-92https://doi.org/10.1111/j.1365-2842.2006.01601.x
[13] Feuerstein, Osnat, Zeichner, Kobi, Imbari, Chen, Ormianer, Zeev, Samet, Nachum, and Weiss, Ervin I. "Temperature changes in dental implants following exposure to hot substances in an ex vivo model." *Clinical Oral Implants Research* 19, no. 6 (2008): 629-633. https://doi.org/10.1111/j.1600-0501.2007.01502.x

[14] Ifayefunmi, O. L. A. W. A. L. E., and Mohd Shahrom Ismail. "An overview of buckling and imperfection of cone-cylinder transition under various loading condition." *Latin American Journal of Solids and Structures* 17 (2020): e329. https://doi.org/10.1590/1679-78256197

[15] Ifayefunmi, O., M. S. Ismail, and M. Z. A. Othman. "Buckling of unstiffened cone-cylinder shells subjected to axial compression and thermal loading." *Ocean Engineering* 225 (2021): 108601. https://doi.org/10.1016/j.oceaneng.2021.108601

[16] Abir, David, and S. V. Nardo. "Thermal buckling of circular cylindrical shells under circumferential temperature gradients." *Journal of the Aerospace Sciences* 26, no. 12 (1959): 803-808. https://doi.org/10.2514/8.8322

[17] Ishak, Muhammad Ikman, Daud, Ruslizam, Bakar, Bakri, and Mohd Noor, Siti Noor Fazliah. "A comparative finite element analysis of regular and topologically optimised dental implants for mechanical and fatigue responses evaluation." *IIUM Engineering Journal* 24, no. 2 (2023): 286 -300. https://doi.org/10.31436/iiumej.v24i2.2695

[18] Ishak, Muhammad Ikman, Daud, Ruslizam, and Mohd Noor, Siti Noor Fazliah. "The effect of material stiffness on dental implant stability – A finite element analysis." *ASEAN Engineering Journal* 13, no. 1 (2023): 59-67. https://doi.org/10.11113/aej.v13.18087

[19] Ishak, Muhammad Ikman, M. U. Rosli, Mohd Riduan Jamalludin, SNA Ahmad Termizi, C. Y. Khor, and M. A. M. Nawi. "Biomechanical assessment of different surgical approaches of zygomatic implant placement on prosthesis stress." In *IOP Conference Series: Materials Science and Engineering*, vol. 932, no. 1, p. 012108. IOP Publishing, 2020. https://doi.org/10.1088/1757-899X/932/1/012108

[20] Yalçın, Mustafa, Kaya, Beyza, Laçin, Nihat, and Arı, Emre. "Three-dimensional finite element analysis of the effect of endosteal implants with different macro designs on stress distribution in different bone qualities." *The International Journal of Oral & Maxillofacial Implants* 34, no. 3 (2019): e43–e50. https://doi.org/10.11607/jomi.7058

[21] Schwitalla, A. D., M. Abou-Emara, T. Spintig, J. Lackmann, and W. D. Müller. "Finite element analysis of the biomechanical effects of PEEK dental implants on the peri-implant bone." *Journal of biomechanics* 48, no. 1 (2015): 1-7. https://doi.org/10.1016/j.jbiomech.2014.11.017

[22] Babayi, Masumeh, and Mohammed N. Ashtiani. "Effects of Cyclic Thermal Loads on Bone-Implant Interface in Dental Prostheses." *Zahedan Journal of Research in Medical Sciences* 19, no. 12 (2017). https://doi.org/10.5812/zjrms.12081

[23] Lin, Min, Xu, Feng, Lu, Tian Jian, and Bai, Bo Feng. "A review of heat transfer in human tooth—Experimental characterization and mathematical modeling." *Dental Materials* 26, no. 6 (2010): 501-513. https://doi.org/10.1016/j.dental.2010.02.009

[24] Ayatollahi, M. R., Yahya, Mohd Yazid, Karimzadeh, A., Nikkhooyifar, M., and Ayob, Amran. "Effects of temperature change and beverage on mechanical and tribological properties of dental restorative composites." *Materials Science and Engineering: C* 54, no. (2015): 69-75. https://doi.org/10.1016/j.msec.2015.05.004

[25] Koutiech, Tammam, Omar Ahmad heshmeh, Kamal Alkerdi, Johnny Toumi, and Laith Al Sabek. "Comparison of Maximum Heat Generation during Implant Site Preparation between Single and Gradual Drilling Protocols in Artificial D1 Bone Blocks: An In Vitro Study." *International Journal of Dentistry* 2022, no. 1 (2022): 9370395. https://doi.org/10.1155/2022/9370395

[26] Gungormus, Mustafa and Erbasar, Guzin Neda Hasanoglu. "Transient heat transfer in dental implants for thermal necrosis-aided implant removal: A 3D finite element analysis." *Journal of Oral Implantology* 45, no. 3 (2019): 196-201. https://doi.org/10.1563/aaid-joi-D-18-00210

[27] Gehrke, Sergio Alexandre, Bettach, Raphaél, Taschieri, Silvio, Boukhris, Gilles, Corbella, Stefano, and Del Fabbro, Massimo. "Temperature changes in cortical bone after implant site preparation using a single bur versus multiple drilling steps: An in vitro investigation." *Clinical Implant Dentistry and Related Research* 17, no. 4 (2015): 700-707. https://doi.org/10.1111/cid.12172